IIETA International Information and Engineering Technology Association
Advancing the World of Information and Engineering

International Journal of Heat and Technology
Vol. 43, No. 1, February, 2025, pp. 228-240
Journal homepage: http://iieta.org/journals/ijht

Optimizing Performance and Emissions of VCR Diesel Engines Using Grey-Taguchi Methods and ANN with Biodiesel from Waste Cooking Soybean Oil

Tejaswita Kajale[1,2*], Jitendra Hole[1], Abhay Pawar[1], Sumit Dubal[3]

[1] Department of Mechanical Engineering, JSPM'S Rajarshi Shahu College of Engineering, Pune 411033, India
[2] Department of Mechanical Engineering, Nutan Maharashtra Institute of Engineering and Technology, Pune 410507, India
[3] School of Automobile Engineering, Symbiosis Skills and Professional University, Pune 412101, India

Corresponding Author Email: tejaswikajale@gmail.com

https://doi.org/10.18280/ijht.430124

Received: 9 December 2024
Revised: 6 February 2025
Accepted: 21 February 2025
Available online: 28 February 2025

Keywords:
waste cooking oil biodiesel, Grey Taguchi, engine emissions, ANN, engine performance

ABSTRACT

This study optimizes diesel engine performance and emissions using biodiesel blends from waste cooking oil. Four blends (10%, 20%, 30%, and 40%) were tested for their impact. The Taguchi design's L16 orthogonal array identified optimal parameters: fuel blend, compression ratio (CR), injection pressure (IP), and injection timing (IT). Key performance metrics such as brake thermal efficiency (BTE), brake power (BP), brake mean effective pressure (BMEP), specific fuel consumption (SFC), and emissions (NOx, CO, HC, CO_2) were optimized using grey analysis. The optimal conditions are 30% biodiesel blend, 18:1 CR, 60 MPa IP, and 25° IT before the top dead center resulting in a 33.3% NOx reduction, 22.5% HC decrease, and 14.06% CO_2 reduction compared to diesel. Despite a 21.21% BSFC increase and 16.85% BTE reduction, biodiesel offers environmental benefits, making it a sustainable alternative for emission reduction. Analysis of variance revealed IP as the most significant factor, contributing 52.20% to the results. Artificial neural network predictions closely matched experimental outcomes, reducing experimental trials. The Grey Taguchi method effectively improved engine performance and reduced emissions. The optimized 30% biodiesel blend significantly lowered NOx and carbon emissions compared to diesel, demonstrating its potential for sustainable biodiesel technology.

1. INTRODUCTION

Growing environmental concerns and the search for sustainable energy alternatives have focused a lot of attention on improving IC engine performance and emissions. we used cooking oil to produce biodiesel, a highly promising alternative fuel due to its renewable characteristics and potential to mitigate emissions of greenhouse gases, among other attributes [1]. However, biodiesel derived from edible oils (such as canola, palm, rapeseed, olive, sunflower, maize, and soybean) is a significant contributor to global food insecurity and expensive prices [2, 3]. However, out of all edible feedstocks, waste cooking oil (WCO) is a viable and potentially cost-effective alternative for biodiesel production [4]. Due to the presence of numerous contaminants (PAHs, PCBs, and dioxin), WCO is readily reusable from residences, hotels, and restaurants that discard it after frying meals [5, 6]. These contaminants pose a threat to the welfare of both animals and humans. Hence, following a pre-treatment procedure, WCO emerges as a viable alternative for biodiesel production while simultaneously addressing the issue of water contamination [6]. Produced from soybean waste cooking oil, biodiesel serves as an environmentally beneficial, cost-effective, and renewable alternative to conventional biodiesel. It addresses environmental and food security concerns by reducing production costs, diverting waste from landfills, and minimizing reliance on virgin vegetable oils, all while substantially reducing greenhouse gas emissions. Soybean oil, a renewable resource, provides a sustainable and consistent feedstock for biodiesel production. In comparison to biodiesel produced from virgin vegetable oils, biodiesel derived from residual cooking oil is a more cost-effective alternative [7-9].

To fully harness the potential of biodiesel blends, this study investigates their performance and emission characteristics under various conditions. This study focuses on optimizing a diesel engine operating at varied input engine parameters and fuel blending with waste-cooking soybean biodiesel blends. The integration of Grey Taguchi methodology and artificial neural networks (ANN) aids in the optimization process, aiming to achieve two key objectives: improving IC engine performance and reducing emissions [10-13]. The Grey Taguchi methodology provides a strong framework for optimizing in the presence of uncertainty through its efficient approach to handling constrained and unreliable data [14, 15]. Compression ratio and injection time highly affect engine performance and emissions [16]. A study by Hirkude et al. [17] looked into how injection timing, injection pressure, and compression ratio (CR) affected the performance and emissions of diesel engines that used a mix of biodiesel from cooking waste and diesel fuel. According to the findings, Enhanced brake thermal efficiency (BTE) alongside reduced brake-specific fuel consumption (BSFC). Although a slight decrease in BTE was observed as BSFC increased when CR was further raised from 18 to 19, this trend aligns with the typical behavior of engine performance characteristics. The optimal conditions for BSFC and BTE were identified at an initial IT of 27° b TDC, 250 bar IP, and a CR of 18. For the fuel that was tested, EGT increased in response to an increase in IP, IT, and CR, while smoke opacity (OP) reduced. Shrivastava and Verma [18] studied the impact of fuel injection pressure and engine load on biodiesel and blends derived from Roselle oil. it was documented that carbon dioxide emissions increased by 1.6% at an injection pressure of 220 bar, whereas smoke and nitrogen oxide emissions decreased by 2.20% and 3.18% respectively, for the RB20 blend in comparison to diesel fuel. Heng Teoh et al. [19] optimized blends of diesel-coconut oil fuel using the grey-Taguchi method (GTM) concerning several parameters, including blend, load, and speed. The optimization result determined the most effective blend ratio, at a speed of 3850 rpm and the load of 25% about the CI engine's emissions, and performance. An optimal configuration of engine load, blend, and speed for a VCR diesel engine was investigated by Gul et al. [13] by utilizing the Taguchi design which operates on pure biodiesel (B100) derived from WCO and a 20% biodiesel and diesel. The primary aim was to attain the most substantial reduction in pollutants and NOx emissions feasible. They used Gray relational analysis to identify the optimal input parameters that would produce desirable output. These parameters include using B100 gasoline, operating at a speed of 2300 rpm, and maintaining a load of 100%. Moreover, the ANOVA approach revealed that the kind of fuel is the primary determining factor, accounting for a significant 44.28% influence on the output parameters. Both the experiment and the artificial neural network (ANN) simulation, which used the expected best combination, confirmed the big improvements in the response factor of the output. This proves the use of the Grey-Taguchi approach for lowering the amount of emissions while simultaneously enhancing combustion and performance. The use of an ANN modeling methodology is effective in determining the necessary output factors when sufficient experimental data is available [20]. Modern neural systems are statistical modeling tools that cater to non-linear input and output data. It is easy to optimize the relationship between input and output parameters. We can conduct optimization studies across all working circumstances by using neural networks for engine predictions [21-23]. Backward feed propagation, when applied to ANN, results in the best possible output. For forecasting outputs, we can make use of MATLAB software along with an artificial neural network [3]. Researchers have conducted several studies on applying the Grey Taguchi technique to optimize engine performance and emission characteristics. In the past, researchers have only looked at the Grey-Taguchi method with a few parameters [24-27]. For example, they looked at waste-cooking biodiesel using the Grey-Taguchi analysis with the BTE performance parameter and the NOx emission parameter. Gul et al. [13] utilized the L9 Taguchi design to optimize fuel type, engine speed, and load for a diesel engine, which alternately fuels with waste cooking oil biodiesel (B100) and a 20% blend of biodiesel with neat diesel (B20). Our research uses a more extensive set of parameters and shows the method's effectiveness in optimizing both performance and emissions simultaneously. ANN was used to predict the responses of the optimized parameters. We compare the ANN-predicted results with the actual experimentation. This approach addresses the limited parameter consideration gap in earlier studies.

2. MATERIAL AND METHODS

In this study, we prepared biodiesel from waste cooking soybean oil using a one-step transesterification process. H_2SO_4 was used as a catalyst. We employed an L16 Taguchi experimental design to alter crucial input parameters such as injection pressure (IP), injection ratio (CR), and injection timing (IT). Additionally, biodiesel blends vary at 10%, 20%, 30%, and 40% concentrations and are named as 10WCO, 20WCO, 30WCO, and 40WCO. Next, we compute the Grey relational grade (GRG) to evaluate the extent of similarity among the performance parameters and the ideal values. Furthermore, the signal-to-noise (S/N) ratio gives significant insights into the quality characteristics under diverse operational conditions. We computed a grey relational grade to evaluate the optimized input combinations. We employed an analysis of variance (ANOVA) to investigate the impact of input parameters on output variables. Finally. We conducted an artificial neural network analysis to validate the optimization technique.

2.1 Characteristics and formulations of fuel

It is especially at risk of contamination when the mixing of biodiesel with diesel is done to produce a blend that is uniform in composition and beneficial for the smooth functioning of unaltered diesel engines. Nevertheless, biodiesel exhibits increased viscosity and density compared with conventional fuel as a result of its increased molecular mass. These characteristics lead to ineffective breakdown and blending. Additionally, it produces a significant amount of carbon dioxide while needing plenty of energy for fuel pumping. The biodiesel, which has a high viscosity, leads to reduced atomization and inadequate evaporation [28]. The physicochemical characteristics of both waste-cooking soybean biodiesel and diesel have been evaluated to determine the compatibility of both in diesel engines. The fuel properties considered are kinematic viscosity, lower calorific value, and density which are carried out as per ASTM standards like D287, D4809, D93-58T, and D445. Table 1 provides the name, make and model of the equipment, as well as the standard for testing fuel blends that were used in the testing. Table 2 depicts the properties of biodiesel blends and diesel.

2.2 Experimental configuration

The equipment utilized in the present investigation is illustrated in Figure 1. In this experiment, a VCR CRDI diesel engine was the equipment utilized in the present investigation as illustrated in Figure 1. In this experiment, a VCR CRDI diesel engine was utilized. Table 3 details the engine specifications. All fuel experiments were conducted within the unaltered engine at ambient temperatures of 298.15 K.

Table 1. Fuel properties test equipments

Equipment Name	Make, Model, Serial No.	Properties Testing	Unit	Standard
Semiautomatic Digital Bomb Calorimeter	HAMCO, HAMCO 6B, Sr.190621	Calorific Value	Cal/gm-°C	IS1350-1966, IP 12/63 T
Cloud and Pour Point Apparatus	HAMCO 9, Sr.190622	Cloud & Pour Point	°C	ASTM D97, IP-15/67
Kinematic Viscosity Bath	HAMCO, 48H2-STD6, Sr.190623	Kinematic Viscosity	cSt or mm^2/sec	ASTM D 445
Pensky Martens Flash Point Apparatus	RICO	Flash Point	°C	ASTM D93-58-T, IS1448, IP 34
Hydrometer	Leimco, M-50SP	Specific Gravity	-	D1448
Biodiesel Preparation Set-Up	Glassware and chemicals	Transesterification Reaction	% Yield	ASTM6751

Table 2. Fuel properties of biodiesel blends

Properties	Unit	B10WCO	B20WCO	B30WCO	B40WCO	B00 Diesel	ASTM Standard
Density at 25°C	kg/m^3	825	828	836	841	816	D287
LCV Calorific Value	Cal/gm	10191	10168	9995	9890	10235	D 4809
Flash Point	°C	66	72	79	81	53	D93-58T
Fire Point	°C	68	74	81	84	56	D93-58T
Kinematic Viscosity @40°C	cSt	2.08	2.21	2.43	2.58	2.09	D445
Dynamic Viscosity @40°C	cP	1.72	1.83	2.03	2.17	1.73	D445

Figure 1. Engine test facility

Table 3. Engine specifications

Make	Kirloskar
Engine Cycle	4-stroke
Rated Speed	1500 rpm
Rated Power	3.5 kilowatts
Type of Dynamometer	Eddy current
Bore Diameter	87.5 millimetres
Stroke Length	110 millimetres
Cooling System	Water cooled
Cubic Capacity	0.661 litres (661 cc)
Ignition System	Compression-Ignition
Compression Ratio	12-18

We conducted experiments on a VCR engine operating at 1500 revolutions per minute, with compression ratios ranging from 15 to 18. The panel box consists of a digital speed indicator, manometer, gasoline tank, air box, digital temperature indicator, and fuel measuring unit. PT100, RTD, and thermocouple sensors are now in stock. Utilize a strain gauge load sensor to measure loads within the range of 0 to 50 kilograms. The engine allows for tilting blocks to shift the compression ratio (CR). The tilting cylinder block setup consists of a tilting block, six Allen bolts, an adjuster to adjust the compression ratio, a locking nut, and an indicator. To adjust the compression ratio, loosen the Allen bolts slightly. After loosening the lock nut, twist the adjuster to set a compression ratio using the indicator and lock it. Gently tighten all Allen bolts. To lower the CR, tilt the block to enhance clearance volume and maintain swept volume. We used a digital voltmeter to measure voltage within the range of 0 to 20 volts. The K-type sensor is used to measure temperature in many zones. We conducted the airflow measurement using an air box. We monitored the cylinder pressure for every one-degree increment in the crank angle. The water flow rate ranges from 40 to 400 liters per hour, whereas the calorimeter flow rate ranges from 25 to 250 liters per hour. A self-priming pump is responsible for circulating water in both the engine and the calorimeter. Conducted tailpipe emissions measurements using a portable AVL Digas 444 gas analyzer. Exhaust emissions from the gas analyzer include HC, CO, NOx, and CO_2.

2.3 Taguchi analysis

Dr. Genichi Taguchi developed a statistical method to minimize process variation through carefully designed experiments. This method uses orthogonal array patterns to speed up the experimental process and provide comprehensive information on every single factor that determines output responses [29, 30]. Taguchi with grey relational analysis (GRA) is the most effective method for analyzing multi-performance characteristics with minimal experimentation [1]. To select an orthogonal array, the control parameters and the number of levels that are related to each factor are taken into consideration. Taguchi organizes quality attributes into three categories by employing a statistical metric known as the signal-to-noise ratio. These categories are as follows: Larger is better, smaller is better, and nominal is the best. On the other hand, Eq. (2) is used to compute the larger-is-better SNR, whereas Eq. (1) is used to estimate the smaller-is-better SNR for lower output responses [31].

$$\mathrm{SNR_s} = -10\log\frac{1}{n}\left\{\sum_{i=1}^{n} y^2{}_i\right\} \quad (1)$$

$$\mathrm{SNR_L} = -10\log\frac{1}{n}\left\{\sum_{i=1}^{n} \frac{1}{y^2{}_i}\right\} \quad (2)$$

In this research, the Larger is better SN ratio was used for BTE, BP, and BMEP While the Smaller is better is used for SFC, NOx, CO, HC, and CO_2. The Grey-Taguchi method has been used for generating a single response based on several performance characteristics. There are four levels for each of the four control parameters: Blend, CR, IP, and IT. The DOF of four factors at four levels is computed by considering the interaction between factors. The levels of the control parameters are detailed in Table 4. L16 represents the orthogonal array that has been chosen for DOE, as illustrated in Table 5.

Table 4. Input controllable parameters with levels

Input Controllable Parameters	Levels			
	L1	L2	L3	L4
Blend ratio of fuel %	B10WCO	B20WCO	B30WCO	B40WCO
Compression ratio	15	16	17	18
Injection Pressure, MPa	30	40	50	60
Injection Timing, °Before TDC	16	19	22	25

Table 5. L16 orthogonal array

Exp. No.	Blend	CR	IP MPa	IT °Before TDC
1	B10WCO	15	30	16
2	B10WCO	16	40	19
3	B10WCO	17	50	22
4	B10WCO	18	60	25
5	B20WCO	15	40	22
6	B20WCO	16	30	25
7	B20WCO	17	60	16
8	B20WCO	18	50	19
9	B30WCO	15	50	25
10	B30WCO	16	60	22
11	B30WCO	17	30	19
12	B30WCO	18	40	16
13	B40WCO	15	60	19
14	B40WCO	16	50	16
15	B40WCO	17	40	25
16	B40WCO	18	30	22

2.4 Grey analysis

Grey relational analysis has been demonstrated as an efficient method for evaluating multi-response optimization problems. Grey relational analysis identifies the crucial aspects of a system and their interrelationships. The critical factors are determined by the sequence of the input and output [32]. Initially, the experimental outcomes were normalized to come within the range of 0 to 1. Next, we calculated the gray relational coefficients from the normalized experimental values. Following this, the GRG was computed using the GRC. The GRG evaluated each of the multiple process responses individually. In this specific case, the process parameters that were considered optimal were the highest GRG values. Eqs. (3) and (4) were used to optimize the initial sequence after adjusting the response parameters by the "larger is better" principle [15].

$$x_i(k) = \frac{y_i(k) - \min y_i(k)}{\max y_i(k) - \min y_i(k)} \quad (3)$$

The initial sequence was optimized as follows when the response parameters were optimized using the "Smaller is better" criterion.

$$x_i(k) = \frac{\max y_i(k) - y_i(k)}{\max y_i(k) - \min y_i(k)} \quad (4)$$

The reference sequence, in this case, $y_i(k)$ is the response's normalized value is $x_i(k)$, and the values of i=1, 2... m are $\min y_i(k)$ and $\max y_i(k)$ respectively, represent the lowest and greatest values of $y_i(k)$

Eq. (5) represents the reference sequence's deviation sequence.

$$\Delta_{0i} = \| x_0(k) - x_i(k) \| \quad (5)$$

Δ_{0i} is called the deviation sequence, $x_0(k)$ is the ideal sequence.

The grey relational coefficient represents the relationship between real experimental data and intended solutions $\zeta_i(k)$. The Eq. (6) is used to calculate it.

$$\zeta_i(k) = \frac{\Delta\min + \Psi\Delta\max}{\Delta_{0i}(k) + \Psi\Delta\max} \quad (6)$$

The maximum and minimum values of the deviation sequences Δ_{0i} are expressed by Δmax and Δmin. The deviation sequence's actual reference is shown by $\Delta_{0i}(k)$ and distinguishing coefficient by Ψ. The value of Ψ always falls between 0 and 1. Generally, $\Psi = 0.5$ is used [33]. Once the GRC has been obtained, the GRG (y_0) is computed.

$$y_0 = \sum_{k=1}^{n} \zeta_i(k)\beta y_i \quad (7)$$

where,

$$\sum \beta = 1 \quad (8)$$

A ranking is given to the experiment set based on the GRG that was found. The optimum combination of inputs in the design of Taguchi is established based on the highest GRG or highest ranking. A greater signal-to-noise ratio (GRG) value is preferable when determining the most optimal set of engine input values based on the average GRG value of all responses at the L16 orthogonal array level. The highest signal-to-noise (S/N) value indicates the optimal level of each input factor.

2.5 ANOVA method

We conducted an ANOVA using Minitab-16 software to determine the proportionate impact of factors that influence the engine's efficiency and exhaust emissions. Furthermore, the input parameter with a higher F-value demonstrates a greater impact on output response [34].

2.6 ANN modelling

Artificial neural network (ANN) is parallel distributed processing units mimic the behaviors of neurons in the human brain, thereby preserving and facilitating access to experimental knowledge at any given moment. The function of these neurons is to encode and retain essential information derived from experimental results via a process of learning and training. Neurons comprising an artificial neural network (ANN) are interconnected through synaptic weights. The synaptic weights determine the necessary outputs or responses for input signals based on the activation function employed, such as tansig or purelin [35]. In MATLAB, the ANN model is constructed utilizing the 'nntool' command. It undergoes training using experimental data to generate predictions for any input parameter combination.

3. RESULTS AND DISCUSSIONS

3.1 Taguchi optimization

To address the issues, we employed the Taguchi technique in addition to grey relational analysis, which incorporates multiple responses. The S/N ratio proved to be the most effective approach for attaining optimal outcomes. The Taguchi technique is the most preferred method for finding the optimum solution with minimal trials. The Taguchi technique measures the standard characteristics using the signal-to-noi**se** quantitative relation (S/N) [36]. The Taguchi approach enhances product quality by prioritizing a mean performance characteristic value that is close to the designated target value rather than one that falls within the specified limits. Figures 2 and 3 present the outcomes of the Taguchi study for the analysis of performance and emission characteristics of engines that include BSFC, BMEP, BTE, BP, NOx, CO, HC, and CO_2. We employ the Taguchi technique for optimization to determine the optimal input parameters. Figures 2(a), 2(b), 2(c), and 2(d) illustrate the analysis of the signal-to-noise ratio for the optimization of BTE, BP, BMEP, and SFC, respectively. The main effects plot shows that B30WCO and B40WCO biodiesel blends have higher SN ratios than other blends across all performance metrics (BTE, BP, and BMEP). These findings suggest they could boost engine efficiency and power. Higher compression ratios also tend to have a positive effect on BTE, BP, and BMEP. On the other hand, for specific fuel consumption (SFC), a lower SN ratio is better. The plot shows that some blends and higher compression ratios may help lower SFC. The study found that the B20WCO blend improved BTE, BP, and BMEP. It achieved the highest BTE when the engine was running at 18 CR, 30 MPa of pressure, and 16°b TDC. The same fuel mixture produced the largest brake pressure when the engine operated at a CR of 16, an IP of 60 MPa, and an IT of 16°b top dead center. To achieve the greatest brake mean effective pressure, the engine should operate on a blend of B20WCO fuel at a CR of 16, with an IP of 60 MPa and an IT of 16 °b TDC. Figures 3(a), 3(b), 3(c), and 3(d) individually exhibit the analysis of the S/N ratio for the optimization of NOx, CO, HC, and CO_2. We apply the "larger is better" criteria to BTE, BP, and BMEP, while we use the "smaller is better" criteria for SFC, NOx, CO, HC, and CO_2. The main effects plot study shows that higher biodiesel blends, particularly B30WCO and B40WCO, tend to have lower SN ratios for NOx, CO, and HC emissions, which could mean less of these pollutants. Also, higher compression ratios tend to lower SN ratios for both NOx and CO, which means they help lower these emissions. However, it's not as clear how the compression ratio changes HC emissions. The opposite is also true: higher biodiesel blends cause higher SN ratios for CO_2 emissions. This is because biodiesel naturally has more carbon content than diesel fuel. Intending to reduce emissions, the blend B30WCO showed the lowest NOx at 18 CR, 50 MPa, and 25°b TDC, while the blend B10WCO revealed the lowest value of CO at 17 CR, 60 MPa, and 25°b TDC. The lowest value of HC is shown by Blend B30WCO at 15 CR, 60 MPa, and 25°b TDC. Blend B30WCO showed the lowest value of CO_2 at 18 CR, 50 MPa, and 25°b TDC. The not-optimal in-cylinder pressure and temperature conditions caused by this compression ratio are responsible for the discrepancy in the signal-to-noise ratios observed at the 17:1 compression ratio. These conditions were not favorable to complete combustion of the biodiesel blend, resulting in reduced performance and emissions signals. This discovery emphasizes the susceptibility of biodiesel combustion to accurate engine configurations. A high CR can enhance BTE by obtaining additional energy from the fuel during combustion. When injected earlier with a high CR, the fuel undergoes more complete combustion, leading to a reduction in HC and CO emissions. ANOVA results indicate that injection pressure is the primary contributing factor. At a high injection pressure of 60 MPa, BTE is higher as a result of better atomization from the high injection pressure, which leads to more complete combustion. The increased oxygen content in WCO biodiesel can result in higher in-cylinder temperatures, which can facilitate the formation of NOx. Figure 3(a) also shows that the higher blends have higher NOx.

3.2 Grey analysis

Table 6 presents the data for 16 experiments (Exp. No. 1 to 16). Each experiment lists the S/N ratio values for each parameter. These values seem to have been normalized, as they all fall within the range of 0 to 1. Table 7 depicts the normalized values, and Table 8 represents the deviation sequence. The deviation sequence calculated after normalization helps determine the degree of similarity between data sequences. Table 9 presents the grey relational grade and ranking. Table 10 probably summarizes the impact of different factors on the average Grey Relational Grade (GRG).

3.3 Anova-based analysis

Furthermore, ANOVA was performed to identify which parameter has a considerable effect on the output of the engine as well as the significance of individual input parameters. By illustrating the interrelationships among these variables, analysis of variance (ANOVA) facilitates the finding of the optimal set of input parameters that optimize engine efficiency and reduce emissions. ANOVA is carried out considering the grey relational grade and the values are presented in Table 11. ANOVA results revealed that the Injection Pressure (IP) is the significant parameter affecting multiresponse with a minimum P value and a contribution of 52.20%. It was found that for the B30WCO blend, BTE increases while SFC decreases with increasing Injection Pressure. This is because atomization works better at higher IP, exposing more of the fuel droplet's surface to the hot air and causing it to completely burn. Figure

2 also reveals that as IP increases, CO decreases, which is the result of complete combustion due to a good-quality fuel mixture. Increasing the injection pressure from 50 to 60 MPa results in an increase in NOx and CO_2. This is because higher injection pressures can improve atomization and mixing, which can improve combustion efficiency. However, higher injection pressures can also result in higher peak temperatures, which can contribute to NOx formation. The amount of oxygen present during combustion influences NOx formation. Increasing injection pressure may alter oxygen availability and affect NOx emissions. The reason for the increase of CO_2 is complete combustion due to high IP which also implies a higher consumption of oxygen, leading to an increase in CO_2 production.

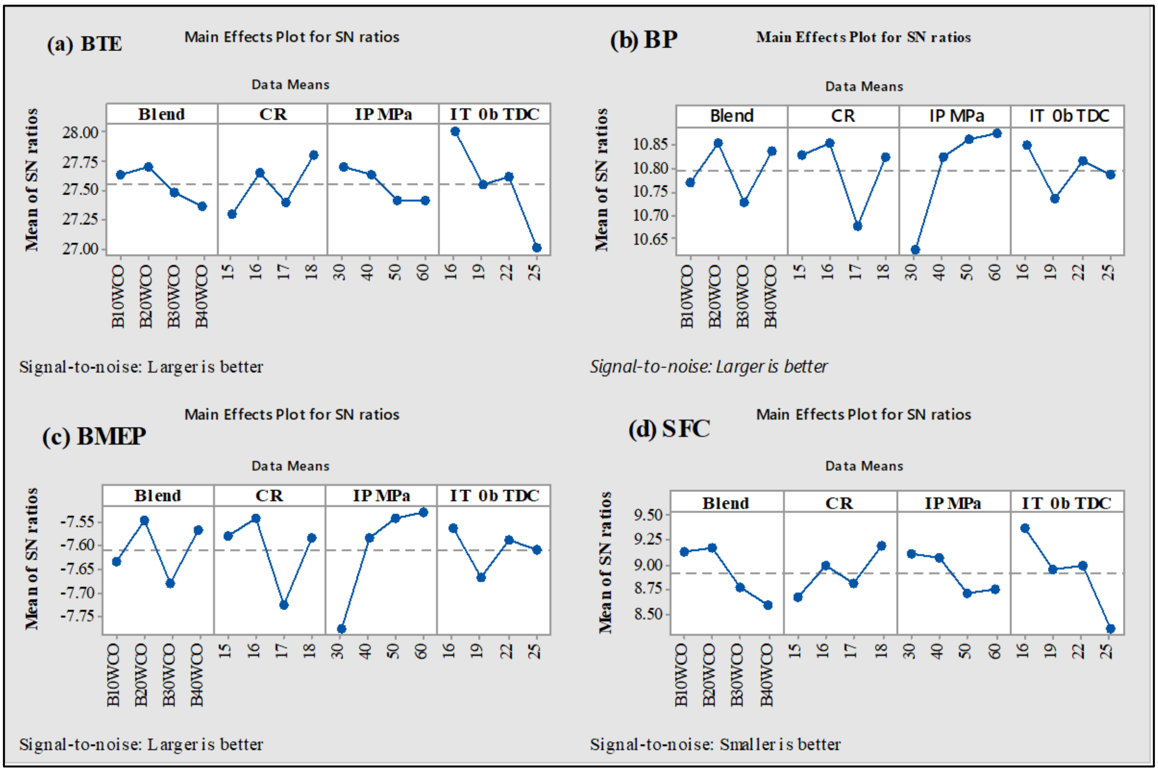

Figure 2. S/N ratio plots for a) BTE, b) BP, c) BMEP, d) SFC

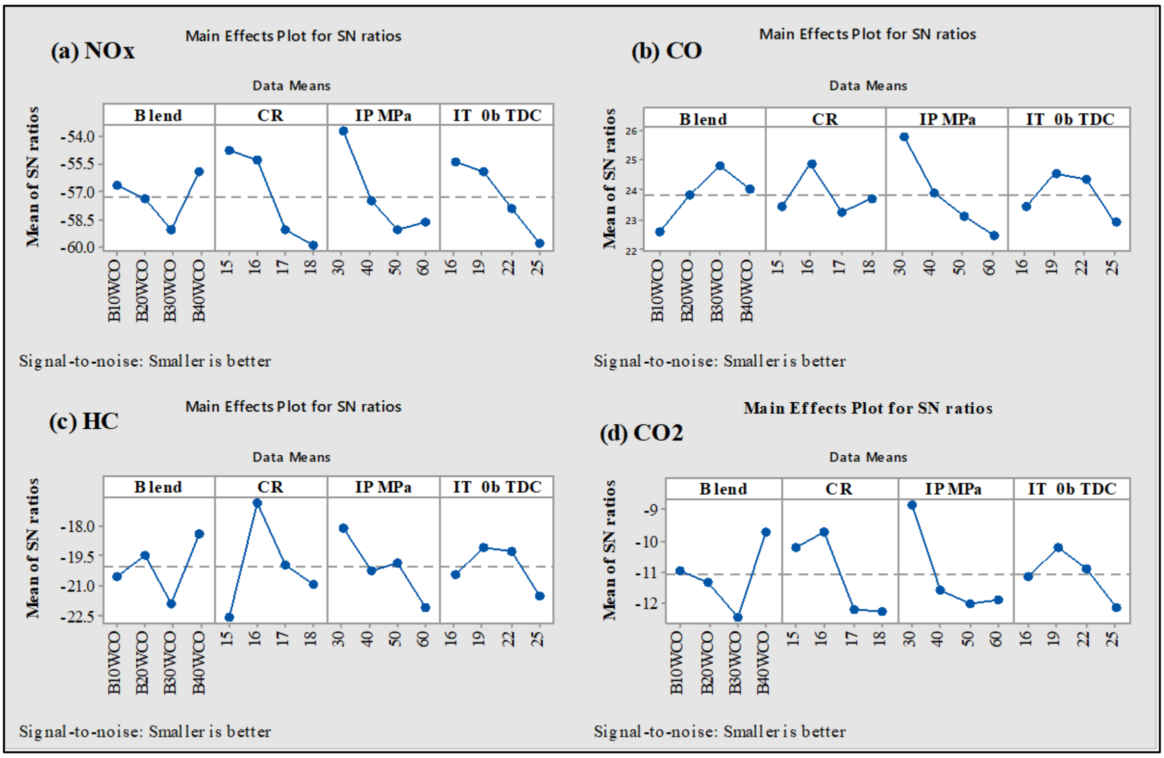

Figure 3. S/N ratio plots for a) NOx, b) CO, c) HC, d) CO_2

Table 6. Signal to noise ratio (S/N ratio)

	Larger is Better				Smaller is Better			
Exp. No.	**BTE %**	**BP kW**	**BMEP MPa**	**SFC Kh/kW**	**NOx ppm**	**CO %**	**HC ppm**	**CO_2 %**
1	28.1035	10.7059	-7.7021	9.6297	-48.1308	23.0980	-22.2789	-7.6042
2	27.7975	10.7564	-7.6390	9.3704	-52.9477	26.0206	-15.5630	-8.2995
3	27.4435	10.7564	-7.6390	8.8739	-61.7343	21.9382	-19.0849	-13.6248
4	27.1891	10.8565	-7.5557	8.6360	-63.9014	19.1721	-25.1055	-14.1514
5	27.5861	10.9309	-7.4938	9.1186	-56.3248	23.0980	-21.5836	-10.8814
6	27.4324	10.7564	-7.6181	8.8739	-55.1327	26.0206	-15.5630	-9.5424
7	27.8539	10.8316	-7.5765	9.3704	-58.0618	23.0980	-20.8279	-12.4650
8	27.9379	10.9061	-7.4938	9.3704	-59.8157	23.0980	-20.0000	-12.2557
9	26.5308	10.7815	-7.6181	7.7443	-60.3072	24.4370	-24.6090	-12.6694
10	27.6439	10.9061	-7.4938	8.8739	-58.5679	24.4370	-20.8279	-11.3640
11	27.4582	10.3703	-8.0461	8.8739	-56.6884	26.0206	-19.0849	-10.6296
12	28.3028	10.8565	-7.5557	9.6297	-60.8672	24.4370	-22.9226	-14.9638
13	27.0127	10.9061	-7.4938	8.1787	-54.0486	23.0980	-21.5836	-9.5424
14	27.7691	11.0046	-7.4118	8.8739	-54.5995	23.0980	-15.5630	-9.5424
15	26.8721	10.7564	-7.6390	8.1787	-59.8599	21.9382	-20.8279	-12.0412
16	27.8187	10.6805	-7.7232	9.1186	-54.9015	27.9588	-15.5630	-7.6042

Table 7. Normalize data

Exp. No.	BTE	BP	BMEP	SFC	NOx	CO	HC	CO_2
1	0.8875	0.5291	0.5424	0.0000	0.0000	0.5532	0.7038	0.0000
2	0.7148	0.6087	0.6418	0.1375	0.3054	0.2206	0.0000	0.0945
3	0.5151	0.6087	0.6418	0.4009	0.8626	0.6852	0.3691	0.8181
4	0.3715	0.7666	0.7731	0.5271	1.0000	1.0000	1.0000	0.8896
5	0.5955	0.8838	0.8708	0.2711	0.5196	0.5532	0.6309	0.4453
6	0.5088	0.6087	0.6747	0.4009	0.4440	0.2206	0.0000	0.2634
7	0.7467	0.7273	0.7404	0.1375	0.6297	0.5532	0.5517	0.6605
8	0.7941	0.8448	0.8708	0.1375	0.7409	0.5532	0.4650	0.6320
9	0.0000	0.6484	0.6747	1.0000	0.7721	0.4008	0.9480	0.6882
10	0.6282	0.8448	0.8708	0.4009	0.6618	0.4008	0.5517	0.5109
11	0.5234	0.0000	0.0000	0.4009	0.5426	0.2206	0.3691	0.4111
12	1.0000	0.7666	0.7731	0.0000	0.8076	0.4008	0.7712	1.0000
13	0.2720	0.8448	0.8708	0.7696	0.3752	0.5532	0.6309	0.2634
14	0.6988	1.0000	1.0000	0.4009	0.4102	0.5532	0.0000	0.2634
15	0.1926	0.6087	0.6418	0.7696	0.7437	0.6852	0.5517	0.6029
16	0.7268	0.4891	0.5091	0.2711	0.4293	0.0000	0.0000	0.0000

Table 8. Deviation sequence

Exp. No.	BTE	BP	BMEP	SFC	NOx	CO	HC	CO_2
1	0.1125	0.4709	0.4576	1.0000	1.0000	0.4468	0.2962	1.0000
2	0.2852	0.3913	0.3582	0.8625	0.6946	0.7794	1.0000	0.9055
3	0.4849	0.3913	0.3582	0.5991	0.1374	0.3148	0.6309	0.1819
4	0.6285	0.2334	0.2269	0.4729	0.0000	0.0000	0.0000	0.1104
5	0.4045	0.1162	0.1292	0.7289	0.4804	0.4468	0.3691	0.5547
6	0.4912	0.3913	0.3253	0.5991	0.5560	0.7794	1.0000	0.7366
7	0.2533	0.2727	0.2596	0.8625	0.3703	0.4468	0.4483	0.3395
8	0.2059	0.1552	0.1292	0.8625	0.2591	0.4468	0.5350	0.3680
9	1.0000	0.3516	0.3253	0.0000	0.2279	0.5992	0.0520	0.3118
10	0.3718	0.1552	0.1292	0.5991	0.3382	0.5992	0.4483	0.4891
11	0.4766	1.0000	1.0000	0.5991	0.4574	0.7794	0.6309	0.5889
12	0.0000	0.2334	0.2269	1.0000	0.1924	0.5992	0.2288	0.0000
13	0.7280	0.1552	0.1292	0.2304	0.6248	0.4468	0.3691	0.7366
14	0.3012	0.0000	0.0000	0.5991	0.5898	0.4468	1.0000	0.7366
15	0.8074	0.3913	0.3582	0.2304	0.2563	0.3148	0.4483	0.3971
16	0.2732	0.5109	0.4909	0.7289	0.5707	1.0000	1.0000	1.0000

3.4 Result validates using ANN

Artificial neural networks (ANNs) enhance the experimental optimization process by predictively optimizing engine performance and emissions. We train artificial neural networks (ANNs), known for their ability to represent complex nonlinear relationships, using experimental data to predict engine behavior under various working conditions. This study employs a feed-forward back propagation network with three neural layers. Input, hidden, and output layers contain four (LOGSIG), ten (LOGSIG), and eight (PURLINE), respectively, neurons. Using eighteen experimental results, the hidden layer number of neurons is determined through trial and continued Continue iterating until the mean squared error between the real experimental data and the expected output data is reduced to its minimum value. The ANN model is trained using the 'Trainlm' function, which adjusts the weight and bias values by Levenberg-Marquardt optimization. We used the ANN model to predict engine performance and emissions due to its ability to efficiently capture complex, nonlinear relationships between input parameters (CR, IP, IT, and load) and output variables. The model's flexibility and predictive accuracy make it ideal for engine setting optimization and emissions improvement in real-world applications.

Figure 4 illustrates a main effects plot for SN ratios. Blend, CR, IP, and IT are the various factors that influence the mean signal-to-noise (SN) ratio. This plot serves as a visual representation of these relationships. SN Ratio: A measure of signal quality relative to noise. A larger SN ratio generally indicates better performance or quality. The factor "Blend" appears to have a significant impact on the SN ratio. B30WCO appears to yield the highest mean SN ratio. Compared to Blend, the effects of CR, IP, and IT on the SN ratio appear less pronounced.

Table 9. Grey relational grade and rank

Exp. No.	BTE	BP	BMEP	SFC	NOx	CO	HC	CO_2	GRG	Rank
1	0.816	0.515	0.522	0.333	0.333	0.528	0.628	0.333	0.501	12
2	0.637	0.561	0.583	0.367	0.419	0.391	0.333	0.356	0.456	14
3	0.508	0.561	0.583	0.455	0.784	0.614	0.442	0.733	0.585	6
4	0.443	0.682	0.688	0.514	1.000	1.000	1.000	0.819	0.768	1
5	0.553	0.811	0.795	0.407	0.510	0.528	0.575	0.474	0.582	8
6	0.504	0.561	0.606	0.455	0.473	0.391	0.333	0.404	0.466	13
7	0.664	0.647	0.658	0.367	0.575	0.528	0.527	0.596	0.570	11
8	0.708	0.763	0.795	0.367	0.659	0.528	0.483	0.576	0.610	4
9	0.333	0.587	0.606	1.000	0.687	0.455	0.906	0.616	0.649	3
10	0.574	0.763	0.795	0.455	0.597	0.455	0.527	0.505	0.584	7
11	0.512	0.333	0.333	0.455	0.522	0.391	0.442	0.459	0.431	16
12	1.000	0.682	0.688	0.333	0.722	0.455	0.686	1.000	0.696	2
13	0.407	0.763	0.795	0.685	0.445	0.528	0.575	0.404	0.575	9
14	0.624	1.000	1.000	0.455	0.459	0.528	0.333	0.404	0.600	5
15	0.382	0.561	0.583	0.685	0.661	0.614	0.527	0.557	0.571	10
16	0.647	0.495	0.505	0.407	0.467	0.333	0.333	0.333	0.440	15

Table 10. Main effect on mean GRG

Factor	Level 1	Level 2	Level 3	Level 4	Max-Min	Rank
Blend	0.5775	0.5569	0.5898	0.5467	0.0431	4
CR	0.5767	0.5265	0.5393	0.6285	0.102	2
IP	0.4595	0.5761	0.611	0.6244	0.1648	1
IT	0.5919	0.518	0.5476	0.6136	0.0956	3

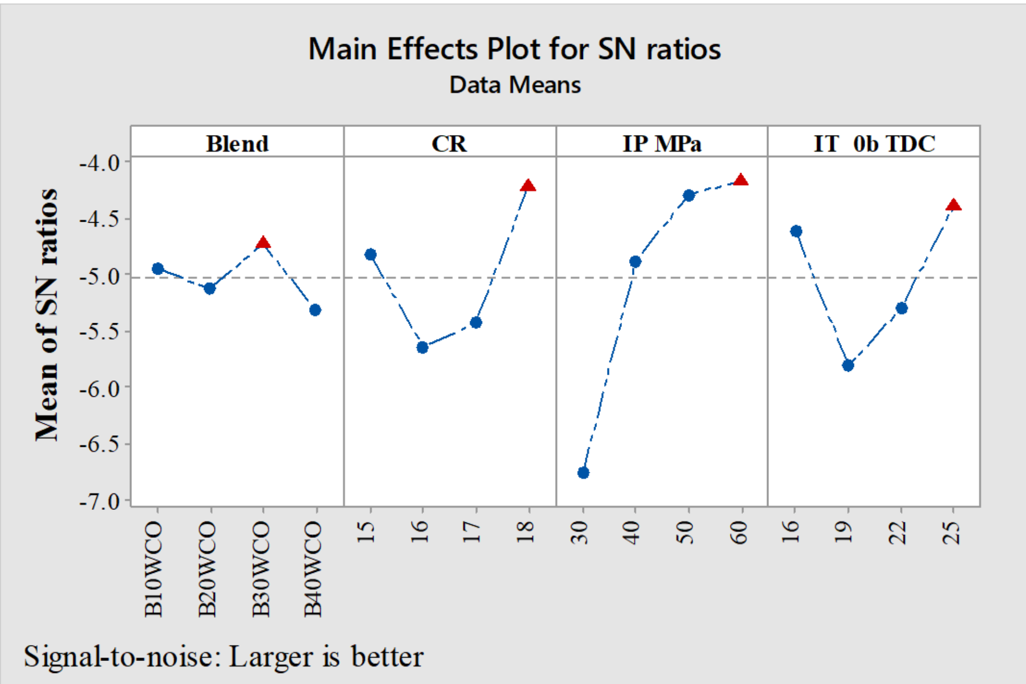

Figure 4. Main effects plot for GRG using S/N ratio

Table 11. Results on ANOVA on grey relational grade

Source	DF	Seq SS	Contribution	Adj SS	Adj MS	F- Value	P-Value
Blend	3	0.004566	3.54%	0.004566	0.001522	0.47	0.727
CR	3	0.025097	19.43%	0.025097	0.008366	2.56	0.23
IP	3	0.067414	52.20%	0.067414	0.022471	6.87	0.074
IT	3	0.022266	17.24%	0.022266	0.007422	2.27	0.259
Error	3	0.009811	7.60%	0.009811	0.00327		
Total	15	0.129155	100.00%				

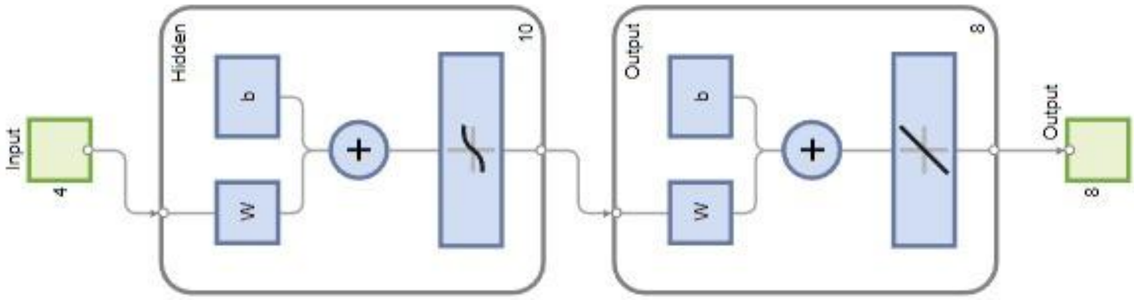

Figure 5. Neural network structure

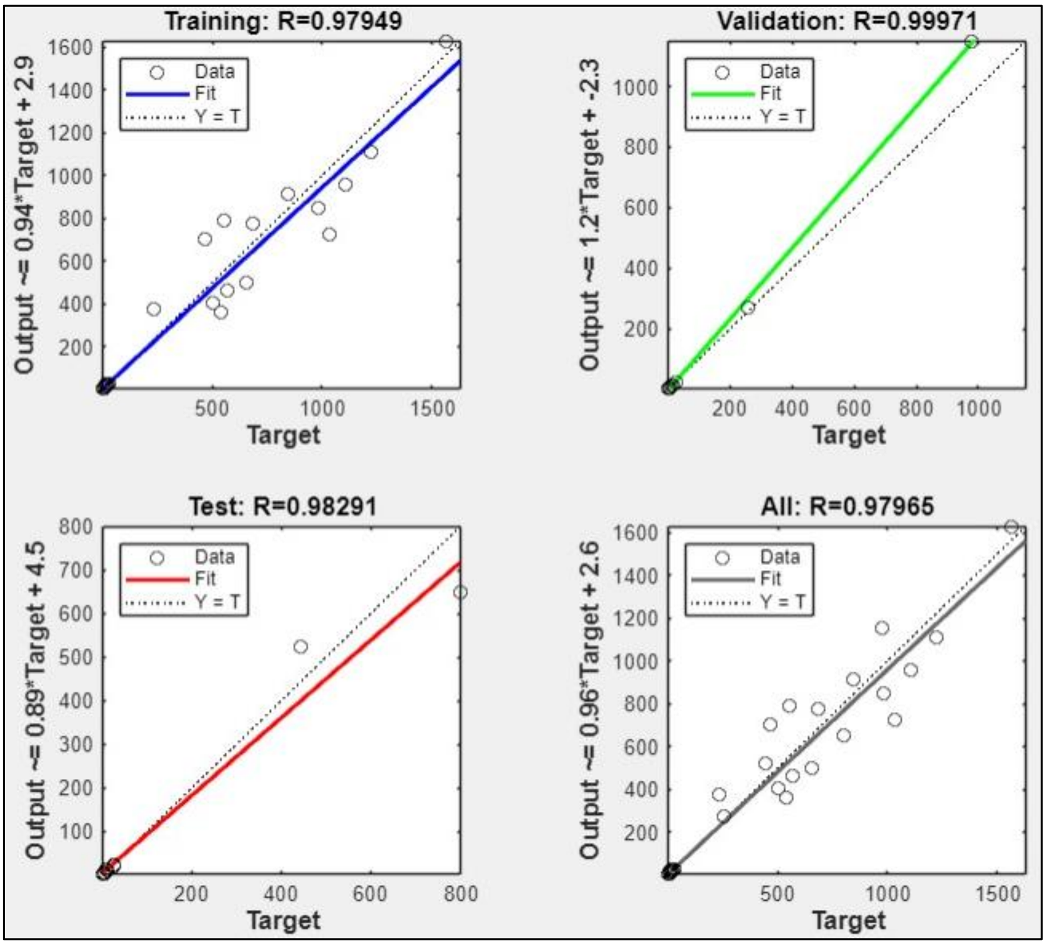

Figure 6. Regression analysis of ANN

Optimizing engine performance and emissions through the interplay of engine operating parameters and the inherent characteristics of biodiesel blends. Injection pressure was found to be the most important parameter, affecting the atomization and mixing of fuel with air. Increased injection pressures facilitate smaller fuel droplets, enhancing a uniform air-fuel mixture and optimizing combustion efficiency. This mechanism is especially evident in the improved Brake Thermal Efficiency (BTE) and lower unburned emissions (CO and HC) observed at elevated injection pressures. The Grey-Taguchi optimization framework effectively addressed the trade-offs between performance metrics and emissions. The fuel properties of biodiesel blends, including viscosity, density, and calorific value, justify the observed trends. The slightly elevated viscosity of biodiesel blends (e.g., 2.43 cSt for B30WCO versus 2.09 cSt for diesel) influences spray formation and penetration, demanding optimal injection pressures to achieve effective atomization. The lower calorific value of biodiesel blends (e.g., 9995 cal/g for B30WCO versus 10235 cal/g for diesel) leads to a higher BSFC, needing additional fuel to achieve comparable power output. Although this, the B30WCO blend exhibited considerable emission reductions of 33.3% in NOx, 22.5% in HC, and 14.06% in CO_2 attributable to the oxygenated characteristics of biodiesel, which optimize the combustion process and reduce incomplete combustion. The analysis underlines the significance of density, which increases with elevated biodiesel content (e.g., 841 kg/m³ for B40WCO versus 816 kg/m³ for diesel). Higher density fuels enhance spray depth but demand precise adjustment of injection timing to prevent excess combustion delays. The flash and fire points of biodiesel blends, which are considerably elevated compared to diesel, enhance safety and stability during operation, rendering biodiesel an acceptable substitute in practical applications.

These findings confirm the optimization process that utilizes the Grey-Taguchi method to determine the optimal parameter combinations. The application of the B30WCO blend in a VCR engine exhibits this balance, showcasing how optimized injection pressures and timing can reduce the limitation of biodiesel's properties while obtaining environmental and performance advantages. Furthermore, the ANN model validated the effectiveness of these optimizations by precisely forecasting the intricate interconnections between engine parameters and results.

Figure 5 depicts this study's architecture of the Artificial Neural Network (ANN) model. The network consists of an input layer with four neurons representing the input parameters: CR, IP, IT, and load. The hidden layer contains 10 neurons, which process the inputs using weighted sums and biases, followed by a non-linear activation function. The output layer has eight neurons corresponding to the predicted engine performance and emission characteristics, including BTE, BP, BMEP, SFC, NOx, CO, HC, and CO_2. The ANN was trained to model the non-linear relationships between input parameters and output metrics, enabling accurate prediction of engine behavior under different operating conditions.

Figure 6 contains a visual representation of the performance of an artificial neural network (ANN) model in predicting a target variable. It contains plots for the training, validation, and testing datasets, as well as critical metrics such as R-squared values and output comparisons. The model's high R^2 values for the training, validation, and testing datasets (0.97949, 0.99971, and 0.98291, respectively) indicate that it has a strong ability for generalization and fits the data well. In all cases, the 'Fit' lines closely follow the 'Data' points, indicating a strong correlation between the predicted and actual values. Figure 7 shows ANN model regression performance in predicting engine performance and emissions. The model inputs are CR, IP, IT, and Load. The outputs are BTE, BP, BMEP, SFC, NOx, CO, HC, and CO_2 emissions. Regression plots show predicted vs. actual results for training (top left), validation (top right), testing (bottom left), and all data combined (bottom right).

3.5 Comparison of results under optimal conditions

The most optimum combination of inputs was determined by the Taguchi-grey method (B30WCO, 18 CR, and IP 60 bar IP and IT 25 °b TDC) was used to compare the diesel and biodiesel response parameters, as illustrated in Figure 8. These results indicate that certain responses to biodiesel were positive, while others were not as favorable when compared to standard diesel. As a result, we observe significant improvements in response outcomes, including emission characteristics. In the meantime, we observe only minor degradation in the responses to engine performance parameters.

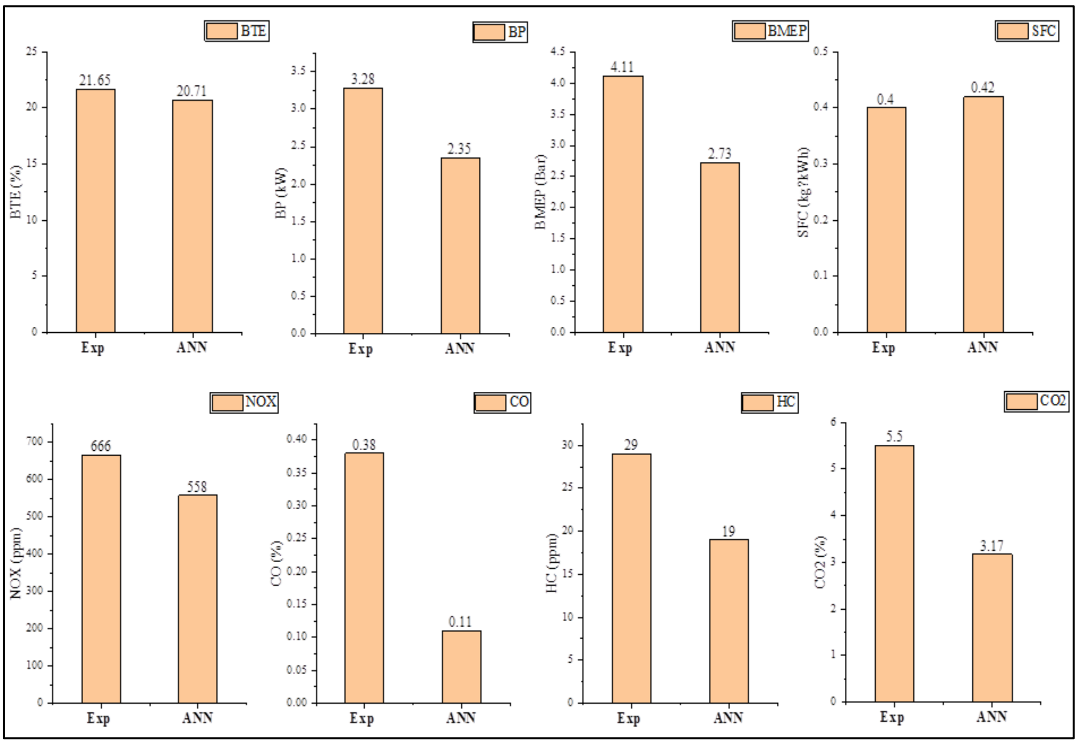

Figure 7. Experimental and ANN predicted results

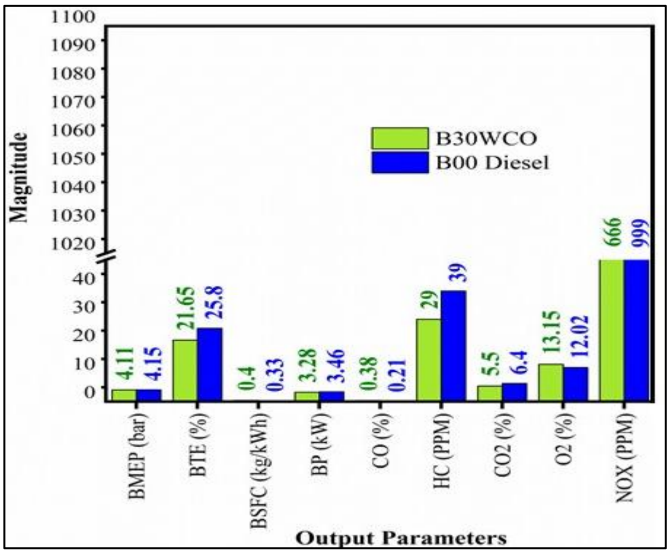

Figure 8. Comparison of engine output parameters

3.6 Experimental and ANN predicted results

We compared the experimental results to the Artificial Neural Network's (ANN) predicted results. The results demonstrate that the ANN methodology can effectively be used to estimate the performance and characteristics of I.C engines. This can be achieved with a reduced number of trials, eliminating the need for a detailed experimental study. As a result, both engineering effort and costs are minimized.

3.7 Uncertainty analysis

In experimental research, statistical analysis of uncertainty is essential because instruments used to measure various parameters are prone to random errors caused by factors such as equipment conditions, laboratory calibration, environmental variables, and reading measurements. Therefore, we use a mathematical expression known as the propagation of errors to minimize the probability of errors occurring. During experiments, equipment errors can help determine the uncertainties in parameter values estimated by instruments. Eq. (9) is utilized to determine the overall percentage uncertainty. Each parameter in the equation contributes to the engine's overall performance and emissions profile. Each parameter's uncertainty reflects the potential variability or measurement error, thereby influencing the reliability of the experimental results.

$$\begin{aligned} &Total\ percentage\ uncertainties \\ &= \sqrt{\begin{bmatrix} (CO)^2 + (NoX)^2 + (HC)^2 + (CO_2)^2 \\ +(BP)^2 + (SFC)^2 \\ +(Pressure)^2 + (Torque)^2 \\ +(Temp)^2 + (Fluid\ flow)^2 \end{bmatrix}} \\ &= \sqrt{\begin{bmatrix} (0.1)^2 + (0.01)^2 + (0.47)^2 + (0.07)^2 + (0.1)^2 \\ +(3.1)^2 + (0.1)^2 + (0.2)^2 + (0.1)^2 + (0.12)^2 \end{bmatrix}} \\ &= \pm 3.15 \end{aligned} \tag{9}$$

It is essential to consider the physical significance of these results to interpret the reliability and accuracy of the experimental results. For example, uncertainties in emissions measurements, influenced by factors such as sensor precision and environmental conditions, indicate the variability in detecting the precise levels of pollutants (CO, NOx, HC, and CO_2). Similarly, uncertainties reflect the sensitivity of engine performance metrics (BP and SFC) to operational conditions, such as fuel quality and engine temperature. The total uncertainty is 3.15%. When making broader generalizations, it is necessary to consider a quantifiable margin of error. The observed trends are statistically significant and robust, as this level of uncertainty confirms. However, it also demonstrates the importance of careful consideration in experimental design and measurement technique precision.

3.8 Comparison of engine output parameters for B30WCO and diesel

B30WCO demonstrated enhanced fuel efficiency in comparison to B00 diesel, as evidenced by its reduced BSFC. In addition, the biodiesel blend exhibited a substantial decrease in hydrocarbon (HC) and carbon monoxide (CO) emissions, suggesting a beneficial environmental effect. Nevertheless, B30WCO exhibited a slight decrease in BMEP and BP, which implies a potential decrease in engine power output. Although the biodiesel blend demonstrated a higher brake thermal efficiency (BTE), indicating improved energy conversion, it also resulted in slightly increased carbon dioxide (CO_2) emissions as a result of its higher carbon content. The substantial increase in nitrogen oxide (NOx) emissions from B30WCO was a critical concern, requiring additional research to develop mitigation strategies.

4. CONCLUSION

The results showed that injection pressure is the most important engine performance factor. A delta value of 0.1648 indicates that it has a greater influence on engine outcomes than other variables. ANOVA shows that injection pressure alone accounts for 52.2% of performance variability, highlighting its importance in engine dynamics. These findings suggest optimizing injection pressure in engine design and operation to improve efficiency and performance.

The blend ratio has a delta value of 0.0431, is less than injection pressure, and has little effect on engine performance. ANOVA shows its negligible contribution compared to key factors like injection pressure. The blend ratio's limited impact suggests that optimizing this parameter alone won't improve engine performance, so focus on more important variables.

By comparing experimental results to those predicted by the ANN, the efficiency of the ANN approach in predicting the performance and emission of IC engines was confirmed.

A comparison of implementing an optimal input combination of biodiesel and diesel demonstrates significant results in lowering exhaust emissions with minimal compromise to performance parameters.

As a method for selecting significant parameters for multi-response variables, the Grey Taguchi strategy was demonstrated to be highly effective. Because it requires less effort, the Taguchi-Grey optimization strategy is recommended for use in industrial applications because it saves time as well as resources.

The investigation's results indicated that the VCR engine may use 30WCO instead of diesel fuel.

Using waste cooking oil biodiesel blends, especially B30, has major environmental advantages. It helps reduce greenhouse gas emissions and waste thereby contributing to a more sustainable energy future. However, when considering the long-term use of these biodiesel blends, it's important to consider potential challenges with engine components and the limited supply of waste cooking oil.

B30WCO blend demonstrated notable environmental advantages with significant reductions in emissions, including a 33.3% decrease in NOx, a 22.5% decrease in HC, and a 14.06% decrease in CO_2 compared to diesel. Despite a 21.21% increase in BSFC and a 16.85% reduction in BTE, these findings affirm biodiesel's potential as a sustainable alternative for applications emphasizing emission control.

REFERENCES

[1] Yaakob, Z., Mohammad, M., Alherbawi, M., Alam, Z., Sopian, K. (2013). Overview of the production of biodiesel from Waste cooking oil. Renewable and Sustainable Energy Reviews, 18: 184-193. https://doi.org/10.1016/j.rser.2012.10.016

[2] Naylor, R.L., Higgins, M.M. (2018). The rise in global biodiesel production: Implications for food security. Global Food Security, 16: 75-84. https://doi.org/10.1016/j.gfs.2017.10.004

[3] Abdolrasol, M.G.M., Hussain, S.M.S., Ustun, T.S., Sarker, M.R., Hannan, M.A., Mohamed, R., Ali, J.A., Mekhilef, S., Milad, A. (2021). Artificial neural networks based optimization techniques: A review. Electronics, 10(21): 2689. https://doi.org/10.3390/electronics10212689

[4] Manikandan, G., Kanna, P.R., Taler, D., Sobota, T. (2023). Review of waste cooking oil (WCO) as a feedstock for biofuel—Indian perspective. Energies, 16(4): 1739. https://doi.org/10.3390/en16041739

[5] Tsai, W.T. (2019). Mandatory recycling of waste cooking oil from residential and commercial sectors in Taiwan. Resources, 8(1): 38. https://doi.org/10.3390/resources8010038

[6] Foo, W., Chia, W.Y., Tang, D., Koay, S., Lim, S.S., Kit Wayne, C. (2021). The conundrum of waste cooking oil: Transforming hazard into energy. Journal of Hazardous Materials, 417: 126129. https://doi.org/10.1016/j.jhazmat.2021.126129

[7] Kajale, T., Pawar, A., Hole, J., Dubal, S. (2024). Selection of optimal waste cooking soybean oil biodiesel blends for emission reduction in CI diesel engines under variable loads: A combined analytic hierarchy process (AHP)-technique for order of preference by similarity to ideal solution (TOPSIS) analysis. International Journal of Automotive Science and Technology, 8(4): 457-466. https://doi.org/10.30939/ijastech.1550536

[8] Wan Osman, W.N.A., Rosli, M.H., Mazli, W.N.A., Samsuri, S. (2024). Comparative review of biodiesel production and purification. Carbon Capture Science & Technology, 13: 100264. https://doi.org/10.1016/j.ccst.2024.100264

[9] Ağbulut, Ü., Sathish, T., Kiong, T.S., Sambath, S., Mahendran, G., Kandavalli, S.R., Sharma, P., Gunasekar, T., Suresh Kumar, P., Saravanan, R. (2024). Production of waste soybean oil biodiesel with various catalysts, and the catalyst role on the CI engine behaviors. Energy, 290: 130157. https://doi.org/10.1016/j.energy.2023.130157

[10] Tuan Hoang, A., Nižetić, S., Chyuan Ong, H., Tarelko, W., Viet Pham, V., Hieu Le, T., Chau, M.Q., Nguyen, X.P. (2021). A review on application of artificial neural network (ANN) for performance and emission characteristics of diesel engine fueled with biodiesel-based fuels. Sustainable Energy Technologies and Assessments, 47: 101416. https://doi.org/10.1016/j.seta.2021.101416

[11] Agrawal, T., Gautam, R., Agrawal, S., Singh, V., Kumar, M., Kumar, S. (2020). Optimization of engine performance parameters and exhaust emissions in compression ignition engine fueled with biodiesel-alcohol blends using Taguchi method, multiple regression and artificial neural network. Sustainable Futures, 2: 100039. https://doi.org/10.1016/j.sftr.2020.100039

[12] Veza, I., Afzal, A., Mujtaba, M.A., Tuan Hoang, A., Balasubramanian, D., Sekar, M., Fattah, I.M.R., Soudagar, M.E.M., EL-Seesy, A.I., Djamari, D.W., Hananto, A.L., Putra, N.R., Tamaldin, N. (2022). Review of artificial neural networks for gasoline, diesel and homogeneous charge compression ignition engine. Alexandria Engineering Journal, 61(11): 8363-8391. https://doi.org/10.1016/j.aej.2022.01.072

[13] Gul, M., Shah, A., Aziz, U., Husnain, N., Abbas, M.M., Kousar, T., Ahmad, R., Hanif, M.F. (2019). Grey-Taguchi and ANN based optimization of a better performing low-emission diesel engine fueled with biodiesel. Energy Sources, Part A: Recovery, Utilization, and Environmental Effects, 44: 1-14. https://doi.org/10.1080/15567036.2019.1638995

[14] Pohit, G., Misra, D. (2013). Optimization of performance and emission characteristics of diesel engine with biodiesel using Grey-Taguchi method. Journal of Engineering, 2013: 1-8. https://doi.org/10.1155/2013/915357

[15] Salmasnia, A., Bastan, M., Moeini, A. (2012). A robust intelligent framework for multiple response statistical optimization problems based on artificial neural network and Taguchi method. Journal of Quality and Reliability Engineering, 2012: e494818. https://doi.org/10.1155/2012/494818

[16] Raheman, H., Ghadge, S.V. (2008). Performance of diesel engine with biodiesel at varying compression ratio and ignition timing. Fuel, 87(12): 2659-2666. https://doi.org/10.1016/j.fuel.2008.03.006

[17] Hirkude, J., Belokar, V., Randhir, J. (2018). Effect of compression ratio, injection pressure and injection timing on performance and smoke emissions of CI engine fuelled with waste fried oil methyl esters - diesel blend. Materials Today: Proceedings, 5(1): 1563-1570. https://doi.org/10.1016/j.matpr.2017.11.247

[18] Shrivastava, P., Verma, T.N. (2020). Effect of fuel injection pressure on the characteristics of CI engine fuelled with biodiesel from Roselle oil. Fuel, 265: 117005. https://doi.org/10.1016/j.fuel.2019.117005

[19] Heng Teoh, Y., Geok How, H., Wen Lee, S., Lin Loo, D., Danh Le, T., Tho Nguyen, H., Sher, F. (2022). Optimization of engine out responses with different biodiesel fuel blends for energy transition. Fuel, 318: 123706. https://doi.org/10.1016/j.fuel.2022.123706

[20] Rathi, N., Rathi, N. (2020). An application of ANN for modeling and optimisation of process parameters of manufacturing process: A review. International Journal of Engineering Applied Sciences and Technology, 4(12):

127-134. https://doi.org/10.33564/IJEAST.2020.v04i12.017
[21] Bhatt, A.N., Shrivastava, N. (2022). Application of artificial neural network for internal combustion engines: A state of the art review. Archives of Computational Methods in Engineering, 29: 897-919. https://doi.org/10.1007/s11831-021-09596-5
[22] Subramanian, K., Sathiyagnanam, A.P., Damodharan, D., Sivashanmugam, N. (2021). Artificial Neural Network based prediction of a direct injected diesel engine performance and emission characteristics powered with biodiesel. Materials Today: Proceedings, 43: 1049-1056. https://doi.org/10.1016/j.matpr.2020.08.015
[23] Fu, J., Yang, R., Li, X., Sun, X., Li, Y., Liu, Z., Zhang, Y., Sunden, B. (2022). Application of artificial neural network to forecast engine performance and emissions of a spark ignition engine. Applied Thermal Engineering, 201: 117749. https://doi.org/10.1016/j.applthermaleng.2021.117749
[24] Mohamed, I.S., Venkatesan, E.P., Parthasarathy, M., Medapati, S.R., Abbas, M., Cuce, E., Shaik, S. (2022). Optimization of performance and emission characteristics of the CI engine fueled with preheated palm oil in blends with diesel fuel. Sustainability, 14(23): 15487. https://doi.org/10.3390/su142315487
[25] Jena, S.P., Mahapatra, S., Acharya, S.K. (2021). Optimization of performance and emission characteristics of a diesel engine fueled with Karanja biodiesel using Grey-Taguchi method. Materials Today: Proceedings, 41: 180-185. https://doi.org/10.1016/j.matpr.2020.08.579
[26] Yessian, S., Varthanan, P.A. (2020). Optimization of performance and emission characteristics of catalytic coated IC engine with biodiesel using Grey-Taguchi method. Scientific Reports, 10: 2129. https://doi.org/10.1038/s41598-019-57129-9
[27] Kumar Rai, R., Rekha Sahoo, R. (2020). Taguchi-Grey method optimization of VCR engine performance and heat losses by using Shorea robusta biodiesel fuel. Fuel, 281: 118399. https://doi.org/10.1016/j.fuel.2020.118399
[28] Hoang, A.T. (2021). Prediction of the density and viscosity of biodiesel and the influence of biodiesel properties on a diesel engine fuel supply system. Journal of Marine Engineering & Technology, 20(5): 299-311. https://doi.org/10.1080/20464177.2018.1532734
[29] Fei, N.C., Mehat, N.M., Kamaruddin, S. (2013). Practical applications of Taguchi method for optimization of processing parameters for plastic injection moulding: A retrospective review. International Scholarly Research Notices, 2013: e462174. https://doi.org/10.1155/2013/462174
[30] Hamzaçebi, C. (2020). Taguchi method as a robust design tool. Quality Control - Intelligent Manufacturing, Robust Design and Charts, IntechOpen. https://doi.org/10.5772/intechopen.94908
[31] Kumar Rai, R., Rekha Sahoo, R. (2020). Taguchi-Grey method optimization of VCR engine performance and heat losses by using Shorea robusta biodiesel fuel. Fuel, 281: 118399. https://doi.org/10.1016/j.fuel.2020.118399
[32] Phanphet, S., Bangphan, S., Bangphan, P., Wangmai, A., Jomjunyong, S. (2022). Applying Grey relational analysis based multi-response optimization of husker process parameters in paddy husking machine. Managing and Implementing the Digital Transformation, 203-213. https://doi.org/10.1007/978-3-031-14317-5_17
[33] Sivaramakrishnan, K., Ravikumar, P. (2014). Optimization of operational parameters on performance and emissions of a diesel engine using biodiesel. International Journal of Environmental Science and Technology, 11: 949-958. https://doi.org/10.1007/s13762-013-0273-5
[34] Benyettou, R., Amroune, S., Slamani, M., Saada, K., Fouad, H., Jawaid, M., Sikdar, S. (2023). Modelling and optimization of the absorption rate of date palm fiber reinforced composite using response surface methodology. Alexandria Engineering Journal, 79: 545-555. https://doi.org/10.1016/j.aej.2023.08.042
[35] Laabid, Z., Moumen, A., Mansouri, K., Siadat, A. (2023). Numerical study of the speed's response of the various intelligent models using the tansig, logsig and purelin activation functions in different layers of artificial neural network. IAES International Journal of Artificial Intelligence (IJ-AI), 12(1): 155-161. https://doi.org/10.11591/ijai.v12.i1.pp155-161
[36] Rashid, K.M.J. (2023). Optimize the Taguchi method, the signal-to-noise ratio, and the sensitivity. International Journal of Statistics and Applied Mathematics, 8(6): 64-70. https://doi.org/10.22271/maths.2023.v8.i6a.1406

NOMENCLATURE

HC	hydrocarbon
NOx	nitrogen oxide
CO_2	carbon dioxide
CO	carbon monoxide
BP	brake power
BMEP	brake mean effective pressure
BTE	brake thermal efficiency
IP	injection pressure
IT	injection timing
CR	compression ratio
S/N ratio	signal-to-noise ratio
GRC	Grey relational coefficient
GRG	Grey relational grade
CR	compression ratio
BOO	diesel
WCO	waste cooking oil
10WCO	10% waste cooking biodiesel with diesel
20WCO	20% waste cooking biodiesel with diesel
30WCO	30% waste cooking biodiesel with diesel
40WCO	40% waste cooking biodiesel with diesel